Dalton Transactions

Accepted Manuscript

ROYAL SOCIETY OF CHEMISTRY

www.rsc.org/dalton

Journal Name

RSCPublishing

ARTICLE

Hydrothermal synthesis, X–ray structure and DFT and magnetic studies of a novel $(H_2SiW_{12}O_{40})^{2-}$ based one–dimensional linear coordination polymer *via in situ* transformation of pyridine–2,3–dicarboxylic acid into nicotinic and 2–hydroxynicotinic acids

Cite this: DOI: 10.1039/x0xx00000x

Received 00th January 2012,
Accepted 00th January 2012

DOI: 10.1039/x0xx00000x

www.rsc.org/

Masoud Mirzaei[a]*, Hoseein Eshtiagh–Hosseini[a]*, Mahboubeh Alipour[a], Antonio Bauzá[b], Joel T. Mague[c], Maria Korabik[d] and Antonio Frontera[b]

In this paper, we report the synthesis and characterization of a novel hybrid inorganic–organic structure formulated as $[[Nd_2(L^1)_2(L^2)(H_2O)_7][H_2SiW_{12}O_{40}]]_n.4H_2O$ (1), in which HL^1= nicotinic acid and H_2L^2=2–hydroxynicotinic acid. Interestingly, L^1 and L^2 are generated from an *in situ* transformation of the original ligand, pyridine–2,3–dicarboxylic acid under hydrothermal conditions. Structural analysis showed this compound is a one–dimensional linear coordination polymer constructed from a repetition of the Keggin anion as a bidentate bridging ligand and one propeller–like dinuclear neodymium complex. Furthermore, in the packing arrangement, hydrogen bonds and anion–π interactions connect the adjacent chains to extend the structure into a 3D architecture. The magnetic properties of this compound also have been studied by measuring its magnetic susceptibility in the temperature range 1.8–300 K. We also analyzed the coordination ability of the SiW12 Keggin anion in reported structures up to now. Finally, we have performed a DFT computational study on the noncovalent anion–π interactions between the Keggin anion and the aromatic ligands coordinated to Nd.

Introduction

In recent years, polyoxometalates (POMs) have shown their competence in being an appropriate building block for constructing inorganic–organic hybrids materials.[1] They either act as a charge–compensating, space–filling, and structure–directing anion,[2] or bond directly to other metals.[3] In the latter case, they are considered as a multidentate ligand, becoming a good target for building various coordination polymers.[4] However, in our recent review, we tried to classify this huge family of compounds and showed POMs can adopt many different coordination modes.[5] We especially focused on Keggin heteropolyanions, because they are more stable and available. So that, we started a systematic study on $SiW_{12}O_{40}^{4-}$ anion recently[6] (henceforth abbreviated as SiW12). Over a hundred X–ray structures are known for hybrids based on SiW12 and an analysis of 183 compounds extracted from 103 scientific papers was carried out to determine the behavior of SiW12 in such systems. Fig. 1 shows how SiW12 uses its surface oxygen atoms to coordinate to other metals. Note that the column corresponding to zero means SiW12 has no covalent connections in 70 compounds and is present just as a counterion. For example, in $[Cu_2(L)_4(H_2O)_2](SiW_{12}O_{40}).8H_2O$, [L = 1,10–(1,4–butanediyl) bis–1H–benzimidazole], SiW12 shows an inorganic template effect for constructing 2D grid–like sheets of four–membered copper circles. The Keggin anions are sandwiched between two neighboring double–sheet units and hydrogen bonding exists between them.[7] On the other hand, SiW12 can adopt 1–9 connecting modes as an inorganic ligand, which may be symmetrical or asymmetrical, although asymmetrical surface modifications are rare.[6,8] A striking example occurred when SiW12 acted as a tridentate pendant ligand covalently bonded to three Cu^I(4,4'–bipy) units through three oxygen atoms of the same W_3O_{13} triad.[8] As we expected, odd numbers of coordination modes are less abundant and in the even numbers, 2 and 4 are more common than others, so that 74% is devoted just to these coordination modes. It is well–known that there are two main structural types of accessible oxygen atoms in POMs: bridging ($M–O_b–M$) and terminal ($M=O_t$) sites which are both potential coordination sites.

Although, SiW12 has 24 O_b and 12 O_t, it frequently uses O_t for coordination, because they are more accessible than O_b. There are 22 reported cases when O_b has been used in conjunction with O_t, usually in high coordination modes. But in a few cases, SiW12 involved only its O_b atoms in coordination sphere.[9] As a rare example, we have a tri–supported Keggin anion, possessing a discrete structure with each of three bridging oxygen atoms of SiW12 coordinated to one $[Cu(en)_2H2O]^{2+}$ fragment in a symmetrical way.[9a]

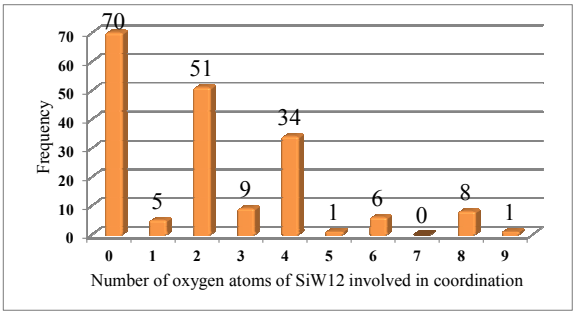

Fig.1 Distribution of different coordination modes of SiW12 anion

Fig. 2 shows the bond length distribution (M–O bond in W–O–M moiety) for 247 recorded bonds. It can be observed that the majority of bonds are in the range of 2.4–2.8 Å, with a mean value of 2.559 Å, which shows the Keggin anion has a relatively weak coordination ability compared to organic ligands. To put this into context, the shortest bond, O_t–Cu: 1.961 Å, has appeared in $[Cu_2(SiW_{12}O_{40})L_1(phen)_2(H_2O)]•3H_2O$, L^1= N,N'–bis(3–pyridinecarboxamide)–1,2–ethane), in which SiW12 behaves as an unsymmetrical tetradentate ligand.[8d] Conversely, the longest bond, O_b–K: 3.343 Å, belongs to $H[KAg_7(4–pytz)_5][SiW_{12}O_{40}]$, pytz = 5–(pyridyl)tetrazolate and SiW12 is considered as an eight–connected node.[10] It is interesting to note that longest bonds are mainly devoted to W–O–M when M is an alkali metal. Moreover, bridging oxygen atoms with a mean value of 2.776 Å for W–O_b–M bonds, often adopt longer bonds ranging from 2.270 to 3.343 Å.

Continuing this approach, we synthesized and characterized a novel neodymium–based inorganic–organic hybrid, formulated as $[Nd_2(L^1)_2(L^2)(H_2O)_7][H_2SiW_{12}O_{40}].4H_2O$ (1), in which L^1= nicotinic acid and L^2 = 2–hydroxy–nicotinic acid. Interestingly, both ligands are generated from the *in situ* decarboxylation and decarbonylation of pyridine–2,3–dicarboxylic acid (2,3–pydc) under hydrothermal conditions. According to the above discussion, the most common coordination mode of SiW12 is bidentate, and in our new compound a symmetrical bidentate mode is also observed. This coordination mode leads to the formation of an unprecedented one–dimensional coordination polymer. In addition, the magnetic properties of this compound are studied herein and the noncovalent interactions responsible for the crystal packing by assembling the infinite 1D polymeric chains are analysed using DFT calculations.

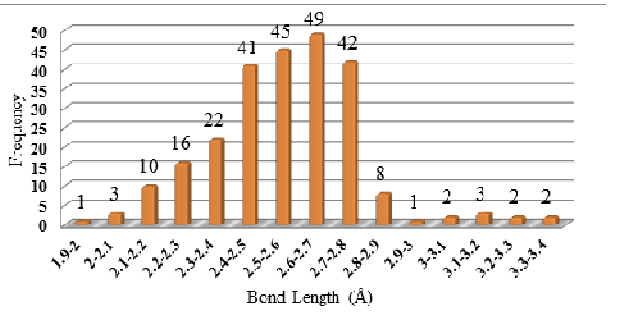

Fig.2 Distribution of bond length attributed to SiW12 ligand

Experimental

General Considerations

All chemicals were commercially purchased and used without further purification. The infrared spectra were recorded in the range of 4000–600 cm^{-1}on a Buck 500 scientific spectrometer as KBr discs. The C, H, and N elemental analysis were performed on Thermo Finnigan Flash model 1112 EA microanalyzer. Thermal gravimetric analysis (TGA) were carried out in an air atmosphere between 20 and 950 °C at a heating rate of 10 °C min^{-1} on a shimadzu Japan TGA–50. Magnetization measurements in the temperature range of 1.8–300 K were carried out for powdered crystals of complexes, at the magnetic field of 0.5 T, using a Quantum Design SQUID Magnetometer (type MPMS–XL5).

Synthesis of hybrid 1

A mixture of $H_4SiW_{12}O_{40}•xH_2O$ (0.1 mmol, 288 mg), $Nd(NO_3)_3•6H_2O$ (0.25 mmol, 110 mg), 2,3–pydc (0.25 mmol, 42 mg) and deionized water (15 ml) was stirred for about 30 min in air. Then NH_4VO_3 (0.1 mmol, 12 mg) was added and the solution was stirred for an extra 30 min. Finally, the pH was adjusted to 2.37 with aqueous NaOH solution. The mixture was then transferred to a Teflon–lined autoclave and kept at 130 °C for 3 days. After slow cooling to room temperature, the solution was filtered off and yellow plate crystals of **1** were obtained by slow evaporation of the filtrate over three days with a 52% yield based on $H_4SiW_{12}O_{40}$. Anal. Calc. for $C_{18}H_{35}N_3Nd_2O_{58}SiW_{12}$: C, 5.77; H, 0.94; N, 1.12%. Found: C, 5.72; H, 0.93; N, 1.13%. IR (KBr pellet, cm−1) ν: 3456(bs), 1648(s), 1596(s), 1566(m), 1466(w), 1411(s), 1374(m), 1318(w), 1229(w), 1014(m), 962(s), 920(s), 888(m), 800(s), 739(m), 674(w).

X–ray Crystallographic Analysis

A yellow, plate–like crystal of **1** was mounted on a nylon loop and placed in the cold nitrogen stream on a Bruker Smart APEX diffractometer. A full sphere of data was collected using a combination of ω and φ scans under control of the APEX2[11] software. The raw data were converted to Fo^2 values with SAINT[11] which also performed a global refinement of unit cell parameters. A numerical absorption correction and merging of

equivalent reflections was performed with SADABS[11] and the structure solved by a combination of Patterson and direct methods (SHELXT[11]). Full–matrix, least–squares refinement of the structure was performed with SHELXL–2014[12] with hydrogen atoms attached to carbon placed in calculated positions and included as riding contributions. Because of the large number of heavy atoms, hydrogen atoms attached to oxygen could not be located with confidence and so are omitted from the model. At initial convergence of the refinement, a pattern of $F_o^2 > F_c^2$ for those reflections showing the worst agreement between the two quantities was evident and application of the TwinRotMat routine in PLATON[13] indicated the presence of a twin component. The refinement was then continued treating the system as a 2–component twin.

Theoretical methods

The energies of the complexes studied herein have been computed at the BP86–D3/def2–TZVP level of theory using the crystallographic by means of the TURBOMOLE 6.4 package.[14] For the study of anion–π complexes of some model systems we have optimized the geometries imposing Cs symmetry. For the calculations we have used the BP86 functional with the latest available correction for dispersion (D3).[15] The NCI analysis has been performed by means of the Non Covalent Interactions Plot software.[16]

Results and discussion

Synthetic considerations

When choosing a ligand, since it was known that lanthanides have a strong tendency to coordinate to O–atoms of carboxylate–containing ligands,[17] we opted for pyridine dicarboxylic acids to construct the hybrid. But compared to other isomers, pyridine–2,3–dicarboxylic acid (2,3–Pydc) is rarely used as a linkage with lanthanides.[18] Searching through literature revealed that this ligand frequently undergoes decarboxylation of the carboxyl group in the ortho position and transforms to nicotinic acid under hydrothermal condition,[19] although there are some instances in which the carboxylate group is retained.[18] *In situ* decarboxylation reaction requires carbon–carbon bond cleavage and is just favoured by the catalytic role of metals.[20] It is important to recognize that only one carboxyl group is lost in this process. In fact, the assistance of one carboxyl group to the departure of the other (by acting as a proton acceptor toward the hydroxyl group of the carboxyl that is lost) is the main reason to why two adjacent carboxyl groups could facilitate elimination of one of them.[20,21] As a result, 2,3 and 3,4 isomers are more disposed to the decarboxylation.[2216] It should be noted that this behavior could be also observed for other isomers of pydc acid, but it is less common.[23] Even with this knowledge, we decided to use this ligand to examine its ability. In POM–based hybrid area, there is only one reported structure using 2,3–pydc, which was conventionally synthesized,[24] so no decarboxylation was observed. This is the first time we introduced 2,3–pydc into such systems under hydrothermal condition and interesting results were obtained. In addition to the formation of nicotinic acid, we also found an unexpected product in the final structure, namely 2–hydroxynicotinic acid. Up to now, oxidative hydroxylation of aromatic rings have been documented for ligands such as 2,2'–bipyridine,[25a] 1,10–phenanthroline[25b] and isophthalic acid[22c] by oxidative agent of Cu^{II} ion under hydrothermal condition. Furthermore, in 1988, Gillard and Hall suggested that the 2 (or 4) position of pyridine becomes polarized upon coordination and can then be oxidized in the presence of dioxygen as oxidant.[26] The most accepted mechanism, known as Gillard mechanism, is defined by nucleophilic attack on the α–carbon atom of pyridine by a hydroxide ion to form a covalent hydrate.[27] In a related work in 2004, Yao et.al could similarly prove that the 2 (or 4) position of nicotinic acid is chemically active and 2–hydroxynicotinic acid might be obtained from nucleophilic substitution reaction between nicotinic acid and OH^- (or source of it, H_2O).[22] Here, the carboxyl group in the 3 position, as an electron withdrawing group, is responsible for reducing the electron density on the pyridyl ring.

Another feature of this synthetic method is the essential role of NH_4VO_3 for successful isolation of the crystal although it is not incorporated into the structure.[4d,10,28] However, when we first ran the reaction without it, some crystals were formed which were not suitable for X–ray analysis. Interestingly, preliminary characterization showed two products are completely different. Our attempts to obtain a suitable single crystal of the first product could be a good clue to compare the two structures to understand the role of NH_4VO_3, as we are intended to do in our laboratory.

IR Spectroscopy and Thermogravimetric study.

The presence of SiW12 is confirmed by characteristic vibration patterns in the IR spectra of **1** in the region with wavenumber lower than 1000 cm^{-1} (Fig. S1). Four bands are attributed to υ(W=Ot), υ(Si=Oa), υ(W=Ob) and υ(W=Oc), which appear at 962, 920, 888, 800/739 cm^{-1}, respectively (where O_a=internal oxygen atoms and O_c=bridging oxygen atoms in the edge–sharing octahedra). Compared with the typical parent anion in $H_4[\alpha–SiW_{12}O_{40}]$, the vibration frequencies of υ(W=O_t) and υ(Si–O_a) have redshifted by 19 and 10 cm^{-1}. This shows that terminal (O_t) and internal oxygen atoms (O_a), which are most affected by interactions with neodymium complexes. On the other hand the vibration frequency of υ(W–O_b) has a blue shift displacement by 8 cm^{-1}. Besides, the υ(W–O_c) vibrational band is splitted into two bands as a consequence of the lower symmetry of the Keggin anion in **1**. In addition, the bands in the range of 1229–1648 cm^{-1} are characteristic of mixed ligands L^1 and L^2.

The thermal stability of compound **1** has been studied by thermogravimetric analysis (TGA) under air atmosphere from 20–950 °C. The plot is depicted in Fig. S2 and the TGA curve exhibits two main stages. Stage 1 is multistep with no stable intermediate and shows 5.35 % weight loss between 20 and 270 °C, which is attributed to the loss of 4 crystalline and 7 coordinated water molecules, and remains in good agreement

with the calculated value of 5.30 %. The 10.70 % weight loss (calculated value: 10.75 %) from 270 to 670 °C is considered to be the release of $2L^1$ and L^2. The total weight loss of 15.71% (calculated, 15.47%) indicates that the final products have $Nd_2SiW_{12}O_{41}$ composition, and this could be either Nd_2O_3+SiO_2+12WO_3 or $Nd_2(WO_4)_3$+SiO_2+9WO_3.

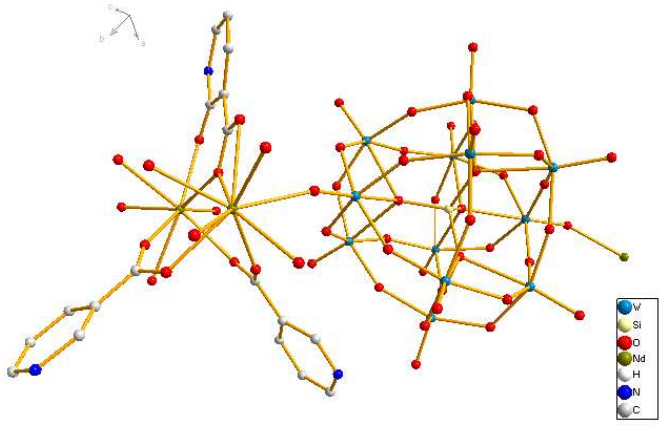

Fig. 3 View of the molecular structure of 1. Lattice water molecules and H atoms are omitted for clarity.

Description of Crystal Structure

Single crystal X–ray structural analysis showed that compound **1** crystallizes in the triclinic space group Pī and the asymmetric unit consists of one SiW12 anion, two Nd(III) ions, two L^1 and one L^2 ligands, seven coordinated and four free lattice water molecules. For the charge balance, two protons are added to the polyoxoanion (Fig. 3) although, as noted above, no hydrogen atoms could be definitively identified in difference maps. Crystallographic data and structural refinements for **1** are listed in Table 1. Selected bond lengths for **1** are also given in Table 1S. Here, three main components of the system will be discussed in more detail.

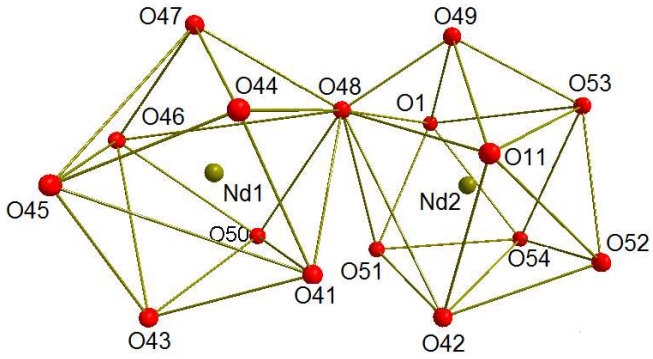

Fig. 4 Polyhedral representation of geometry around dinuclear neodymium complex in 1

Table 1. Crystallographic Data and Structure Refinement for 1

empirical formula	$C_{18}H_{35}N_3Nd_2O_{58}SiW_{12}$
formula weight	3744.1
temperature (*K*)	150(2)
crystal size (mm^3)	0.027 × 0.107 × 0.174 0.020 × 0.045 × 0.095
crystal system	triclinic
space group	*P*ī
a (Å)	12.6060(19)
b (Å)	12.9593(19)
c (Å)	18.631(3)
α (°)	82.317(2)
β (°)	88.815(2)
γ (°)	71.173(2)
V (Å3)	2854.2(7)
Z	2
*D*calc (g cm–3)	4.310
θ Range (°)	1.675-26.940
μ (mm^{-1})	26.000
F(000)	3236
reflections collected	44800
final *R*1[a], *wR*2[b] [*I* > 2 σ(*I*)]	0.0642, 0.1480
GOF	1.035

a $R1 = \Sigma||F_o| - |F_c||/\Sigma|F_o|$. b $wR_2 = \{\Sigma w(F_o^2 - F_c^2)^2/ \Sigma w(F_o^2)^2\}^{1/2}$.

In the dinuclear neodymium cation, there are two crystallography independent Nd(III) ions with different coordination environments. They share a corner and are bridged by a carboxylate oxygen atom (O48) belonging to the L^2 ligand (Fig. 4). Nd1 is eight–coordinated with a square antiprismatic geometry (NdO_8), being coordinated by four O atoms from three different ligands (Nd–$O_{carboxylate}$: 2.37(2) – 2.40(2) Å) and four O atoms from four water molecules (Nd–O_{water}: 2.44(2) – 2.61(2) Å). In the coordination polyhedron around Nd1, the O41, O43, O44, O45 group and the O46, O47, O48, O50 group define two bottom planes of the square antiprism with a dihedral angle of 3.16º between these two planes. The distances between Nd1 and the two bottom planes are 1.390 and 1.282 Å, respectively (Fig. S2a). These data indicate that the square antiprismatic geometry of Nd1 is distorted. On the other hand, Nd2 is nine–coordinated and adopts a distorted tricapped trigonal prismatic geometry (NdO_9), which is defined by four O atoms from three different ligands (Nd–$O_{carboxylate}$: 2.40(2) – 2.57(1) Å), two O atoms from two different SiW12 (Nd–$OSiW_{12}$: 2.47(1), 2.55(1) Å) and four O atoms from three water molecules (Nd–O_{water}: 2.48(2) – 2.53(2) Å). In the coordination polyhedron of Nd2, the O1, O53, O54 group and the O11, O42, O48 group constitute the two bottom surfaces of the trigonal prism and the dihedral angle between these two planes is 12.18° and the distances between Nd2 and the two bottom planes are 1.742 and 1.577 Å, respectively. The O1, O11, O48, O53 group, O1, O42, O48, O54 group and O11, O42, O53, O54 group form the three side planes of the trigonal prism. The distances between the Nd2 and the three side planes are 1.088, 0.716 and 0.834 Å, respectively. In addition, the O49, O51 and O52 atoms occupy the three cap positions and the distance between them and the relevant side plane are 1.438, 1.681, 1.659 Å, respectively (Fig. S2b). The above–mentioned data also confirm the distortion in the bicapped trigonal prism. The Nd1···Nd2 distance is 4.297 Å, which is shorter than the sum

of the Van der Waals radius of two Nd atoms (4.58 Å). Furthermore, this moiety connects SiW12 units through terminal oxo groups that are just positioned at opposite sides of the Keggin core forming a linear 1D chain with a repeating unit of [−{Nd2}−POM−] (Fig. 5a). Notably, only Nd2 is responsible for constructing the polymer chains and Nd1 can be considered as a pendant group (Fig. 5b).

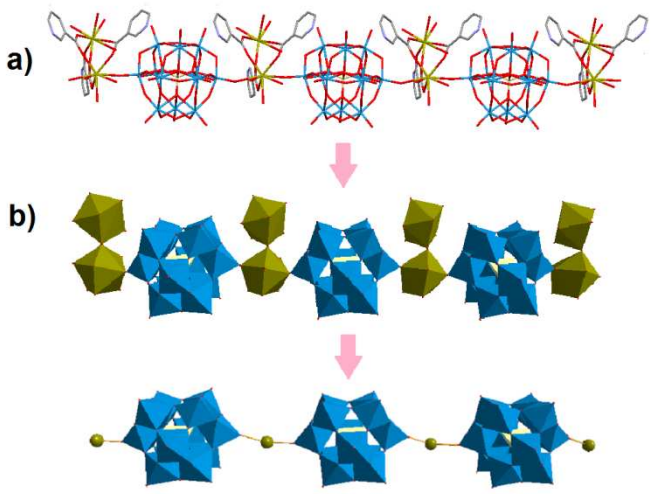

Fig. 5 Representation of 1D chain structure in 1. The hydrogen atoms are omitted for clarity.

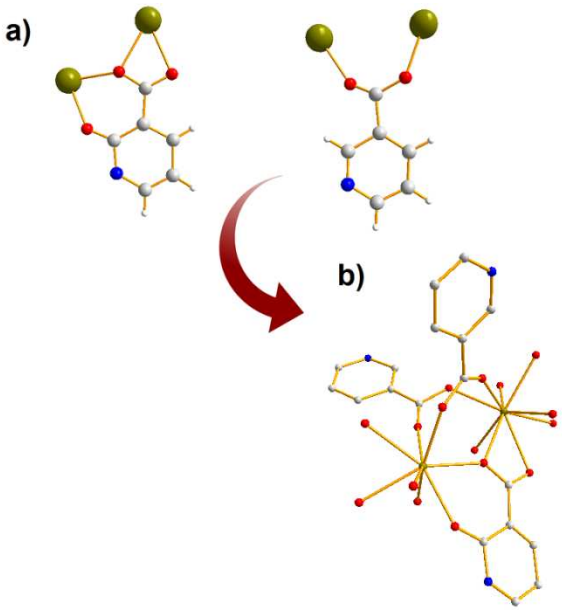

Fig. 6 a) Coordination modes of ligand L1 and L2. b) Structure of the dinuclear unit in 1. (H atoms are omitted for clarity)

Bridged neodymium atoms by nicotinic acid ligands are a very common motif.[20b,29] As we know, nicotinic acid could be both chelating[30] and bridging[31] ligand via its carboxylate moiety. But in a bridging mode, it has proved that is a good candidate for obtaining dinuclear complexes, especially when it is treated with lanthanides.[29,32] Here, each L^1 ligand acts as a $\mu_2(\eta^1, \eta^1)$–bridging ligand via its carboxylate group in a bidentate fashion (Fig. 6a). On the other hand coordination mode of L^2 is also interesting and is only observed in a few cases.[33] It is considered as a tridentate ligand with $\mu_2(\eta^2, \eta^2)$–bridging mode of carboxylate and hydroxyl group in adjacent positions (Fig. 6a). Interestingly, in both ligands, the nitrogen atom of pyridine rings does not have any tendency toward coordination to Nd atoms (Fig. 6b).

The structure of the well–known SiW12 Keggin core includes a central $\{SiO_4\}$ tetrahedron surrounded by twelve $\{WO_6\}$ octahedra arranged in four groups of three edge–sharing octahedral units $\{W_3O_{13}\}$. Each of the trinuclear units share corners with each other and are disposed tetrahedrally around the central Si atom with Si–O distances of 1.62(2) Å. As we explained above, SiW12 offers two O_t atoms to coordinate to two Nd atoms in a symmetrical bidentate coordination mode (Fig. S3) and form a 1D linear polymeric chain. In fact, here, the organic ligands do not play any role in constructing the polymer chains and only SiW12 exerts its linkage role. Based on the results obtained in the introduction section, this is the most frequent observed coordination mode of SiW12 and the bond lengths (Nd2–O11 = 2.47(1), Nd2–O1 = 2.55(1) Å) are in the expected range. As shown in Fig. S4, two adjacent SiW12 units are separated by the propeller–like, dinuclear complex of Nd at a distance of 14.880 Å for Si–Si. A noteworthy feature of **1** is that the polymeric chains are linked to the neighboring chains via hydrogen bonding and anion–π interactions, as if the SiW12 is encapsulated in a group of aromatic rings. This fact is illustrated in Fig. 7, in which O33, one of the bridging oxygen atoms of SiW12, is oriented toward the π–face of pyridine ring of neighboring unit by distance of 3.012, indicating a strong interaction.

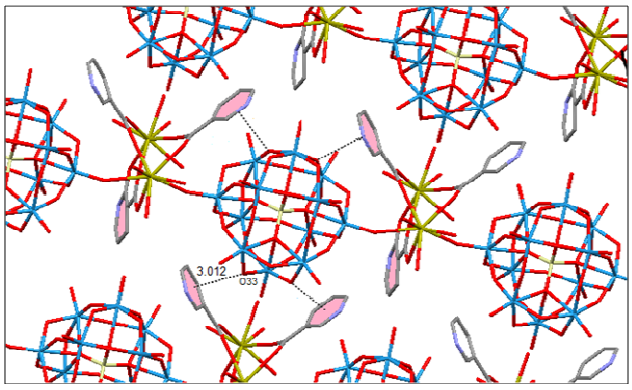

Fig.7 Indication of anion–π interaction established between organic ligands and surface oxygen atoms of SiW12 anion

Magnetic properties.

Magnetization measurements in the temperature range of 1.8 – 300 K have been carried out for powdered crystals of compound; at the magnetic field of 0.5 T. Corrections for diamagnetism of the constituting atoms have been calculated using Pascal's constants.[34] The effective magnetic moments

have been calculated from the following expression: $\mu_{eff} = 2.83(\chi_{mcorr} \times T)^{1/2}$ (B.M.).

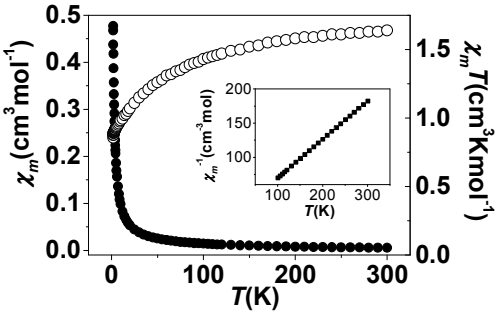

Fig.8. Variable–temperature magnetic susceptibility in the form of χm(●) and χmT (○) versus T, (χm calculated per 1 NdIII center). The insets show the temperature dependence of reciprocal magnetic susceptibility.

The temperature variation of the magnetic susceptibility χ_m and of χ_mT product of the Nd^{III} compound is displayed in Fig. 8. The experimental room temperature χ_mT value 1.65 cm^3 K mol^{-1} (μ_{eff} =3.64 B.M.) is equal to the theoretical one (χ_mT = 1.64 cm3 K mol−1) for Nd^{III} ion. For Nd^{III} ion, S = 3/2, L = 6, g = 8/11 and the ground state is $^4I_{9/2}$.[6b,34b,35] On cooling, χ_mT values gradually decreases, the χ_m^{-1} versus T data obey the Curie−Weiss law in the range 100−300 K (Fig. 8 inset), with C=1.78cm^3 K mol^{-1}. Similar behavior, typical of isolated Nd^{III} coordination compounds, we presented recently.[6b] The ground state of free Nd^{III} ion is populated only, even at room temperature, because the first excited state is located at above ca 2000 cm^{-1} (1400 K).[6b,34b,35] Below 100 K a steeper decrease of χ_mT is observed, as a combination effect of thermal population of the Stark levels, modulated by the crystal field and the molecular symmetry of the compound. Similar behavior ($\chi_m T$vs.T relations) of dimeric Nd^{III} [35d,f,g], trinuclear[6b] as well as of ZnNd[34g] complexes were recently observed by other Authors. Very small value of exchange interactions, zJ' =-0.06 cm^{-1} was calculated for dimeric complex, with Nd^{III} ions connected by two oxygen in the distance of 3.9944 Å.[35f] Magnetism presented for ZnNd complex[35g] and similar (in the range) decrease of $\chi_m T$ at low temperatures could be treated as corresponding to isolated, monomeric Nd^{III} complex (Zn^{II} ion is diamagnetic). These examples confirm that in dimeric complex analysed by us, decrease of $\chi_m T$ curves is typical of the thermal depopulation of the Stark components that results from the crystal field effect. Exchange interaction within such dimeric units could be rather small, however the distance between Nd^{III} ions is short. Some information on the nature of exchange interaction could be extracted from magnetization measurements (Fig. S6). Tendency to saturation is observed in magnetization $M/N\beta$ curve at 2K, to the value 1.58 $N\beta$, corresponding well to the fundamental Kramer doublet of Nd(III) ion, with S=1/2 at 2K.[34b]

Theoretical study.

We have divided the theoretical study into two parts. First, inspired by the solid state architecture of compound **1** (see Fig. 9A), we have envisaged a simple model to analyze the ability of coordinated nicotinic acid to interact with anions by means of anion–π interactions. That is, the polymeric chains of **1** aggregate in the solid state by means of multiple anion–π interactions between the $[H_2SiW_2O_{40}]^{2-}$ anionic moieties and two aromatic ligands of the cationic $[Nd_2(L^1)(L^2)(H_2O)_7]^{2+}$ moieties. Therefore, we have designed a neutral model system (M) mimicking this system where two transition metal ions (Zn^{2+}), two nicotinic ligands and one coordinated carbonate counterion form the anion receptor. We have optimized two complexes (see Fig. 10), using a dianion (carbonate) and monoanion (azide) to study the ability of this receptor to bind anions by means of anion–π interactions involving the aromatic ligands and analyze the influence of the charge of the anion on the interaction energy. It can be observed that the carbonate complex shows a very strong interaction energy (ΔE_1 = –91.7 kcal/mol) and a more modest one for azide (ΔE_2 = –22.9 kcal/mol). The computed equilibrium distances are shorter for the $M\cdots CO_3^{2-}$ anion in line with the interaction energy. Moreover, the anion–π interaction is mainly established between the azide/carbonate anion and the exocyclic C–C bond connecting the carboxylate group to the ring.

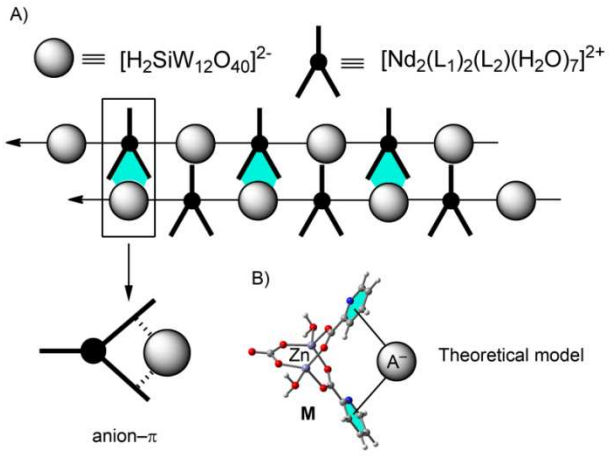

Fig.9 Schematic representation of the solid state architecture of compound 1 and the theoretical model (M).

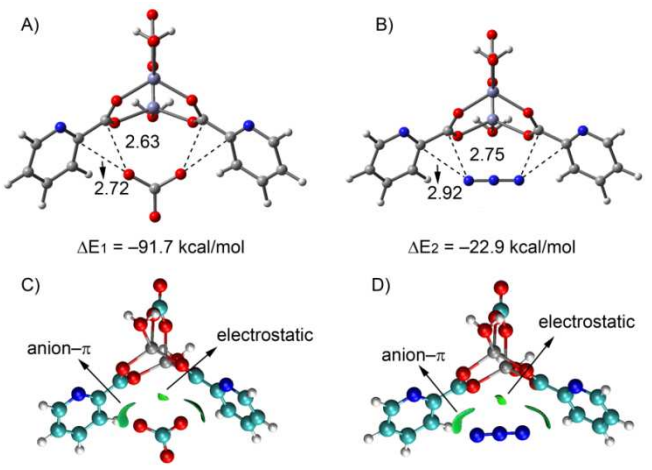

Fig.10 Optimized complexes and NCI plots. Distances in Å.

We have used the NCI plot (see Fig. 10) to characterize the anion–π interactions described above for the theoretical model. This method uses a visualization index based on electron density and its derivatives, and enables the identification and visualization of noncovalent interactions efficiently. The isosurfaces correspond to both favorable and unfavorable interactions, as differentiated by the sign of the second density Hessian eigenvalue and defined by the isosurface color. NCI analysis allows an assessment of host–guest complementarity and the extent to which weak interactions stabilize a complex. The green color of the isosurfaces indicates a favorable interaction, in agreement with the energetic study. In addition, the shape of the surfaces that characterize the anion–π interactions in both complexes (see C and D in Fig. 10) confirms that the interaction is basically with the exocyclic C–C bond. The NCI plots also show a small isosurface that represents the purely electrostatic interaction between the metal ions and the interacting anion.

In the second part of the theoretical study we have analyzed a monomeric part of the infinite chain of compound **1** (see Fig. 11A) using the crystallographic coordinates. In Fig. 11B we show the theoretical model used where we have added two hydrogen atoms to the oxygen atoms that connect the $[Nd_2(L^1)(L^2)(H_2O)_7]^{2+}$ moieties to the $[H_2SiW_2O_{40}]^{2-}$ anionic counterparts. Therefore the Nd2 part of the complex is neutral. This allows us to evaluate the interaction without the contribution of strong electrostatic effects. It can be observed that one oxygen atom of the $[H_2SiW_2O_{40}]^{2-}$ moiety is located approximately in the center of the aromatic cleft interacting with the exocyclic CC bonds in agreement with the location of the anion in the model complexes described in Fig. 9. Moreover, additional oxygen atoms of the $[H_2SiW_2O_{40}]^{2-}$ anion also interact with the aromatic ring. The interaction energy is large and negative (ΔE_3 = –50.6 kcal/mol) indicating a strong binding. The NCI plot (see Fig. 11C) shows large isosurfaces that characterize the anion–π interactions. It can be observed that the surface is extended through the entire aromatic systems, indicating a good complementarity between the coordinated nicotinic ligands and the Keggin anion. There is also an small and circular region that corresponds to a hydrogen bonding interaction between a coordinated water molecule of the $[Nd_2(L^1)(L^2)(H_2O)_7]$ moiety and the anion. Finally, a direct interaction between the oxygen atom of the anion that points to the center of the aromatic cleft and Nd atoms can be also appreciated in the NCI plot.

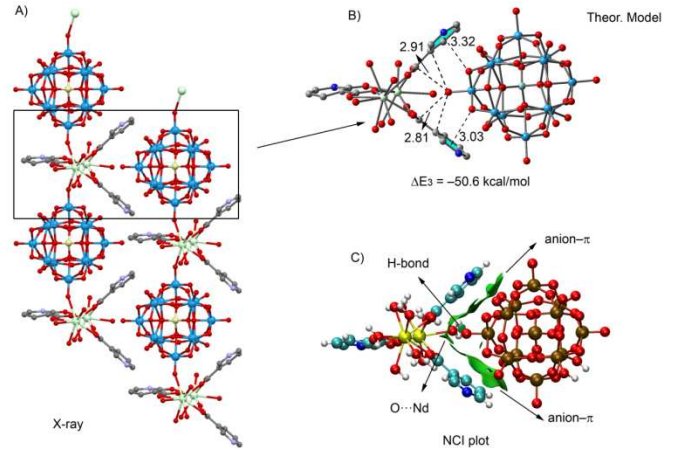

Fig.11 A) Fragment of the crystal packing of 1. B) fragment used to evaluate the anion–π interaction. C) and the NCI plot of the theoretical model. Distances in Å.

Conclusion.

In summary, we report the synthesis and X–ray characterization of one new hybrid based on Keggin polyoxometalate and rare earth metal. The structure consists of dinuclear neodymium complexes which are further connected by the Keggin inorganic building block. Here, the Keggin anion acts as a bidentate bridging ligand, leading to the formation of a 1D linear polymeric chain. Supramolecular interactions such as hydrogen bonds and anion–π interactions could enhance the stability of compound **1**. One interesting feature of this synthesis was the *in situ* transformation of pyridine–2,3–dicarboxylic acid during the course of hydrothermal treatment. Although we used 2,3–pydc as the original ligand in the preparation of hybrid **1**, nicotinic acid and 2–hydroxynicotinic acid were unexpectedly found in the final product. These observations confirm that the hydrothermal technique has some intriguing and unexpected results that need further investigation and we expect that this technique will attract the attention of the scientific community. We have also reviewed the SiW12 anion behaviour in hybrid systems and concluded that the bidentate coordination mode is preferred over other possibilities.

Supporting Information

Additional figures, IR spectra and TG/DTA curves are available in supporting information section.

CCDC 1040276 for 1 contains the supplementary crystallographic data for this paper. These data can be obtained free of charge from The Cambridge Crystallographic Data Centre via www.ccdc.cam.ac.uk/data_request/cif.

Acknowledgements

MM and HEH would like to thank the Ferdowsi University of Mashhad for financial supporting of this study (Grant no. 28395/3–2013/10/02). AF and AB thank the DGICYT of Spain (projects CTQ2011–27512/BQU and CONSOLIDER INGENIO 2010 CSD2010–00065, FEDER funds) and the Direcció General de Recerca i Innovació del Govern Balear (project 23/2011, FEDER funds) for financial support. JTM thanks Tulane University for support of the Tulane Crystallography Laboratory. We thank the CTI (UIB) for free allocation of computer time.

Notes and references

[a]Department of Chemistry, Ferdowsi University of Mashhad, Mashhad 917751436, Iran, E–mail: mirzaeesh@um.ac.ir; heshtiagh@um.ac.ir
[b]Departament de Química, Universitat de les Illes Balears, Crta. de Valldemossa km 7.5, Palma de Mallorca, Baleares E–07122, Spain.
[c]Department of Chemistry, Tulane University, New Orleans, Louisiana 70118, United States
[d]Faculty of Chemistry, University of Wrocław, F. Joliot–Curie 14, 50–383 Wrocław, Poland

Electronic Supplementary Information (ESI) available: [details of any supplementary information available should be included here]. See DOI: 10.1039/b000000x/

1 (a) A. Dolbecq, E. Dumas, C. R. Mayer, P. Mialane, *Chem. Rev.,* 2010, 110, 6009. (b) D. L. Long, R. Tsunashima, L. Cronin, *Angew. Chem., Int. Ed.,* 2010, 49, 1736. (c) H. N. Miras, J. Yan, D. L. Long, L. Cronin, *Chem. Soc. Rev.,* 2010, **41**, 7403. (d) F. Li, L. Xu, *Dalton Trans.,* 2011, **40**, 4024. (e) Y. F. Song, R. Tsunashima, *Chem. Soc. Rev.,* 2012, **41**, 7384.

2 (a) D. Y. Du, J. S. Qin, S. L. Li, Z. M. Su, Y. Q. Lan, *Chem. Soc. Rev.,* 2014, 43, 4615. (b) X. J. Kong, Y. P. Ren, P. Q. Zheng, Y. X. Long, L. S. Long, R. B. Huang, L. S. Zheng, *Inorg. Chem.,* 2006, **45**, 10702. (c) K. Uehara, K. Kasai, N. Mizuno, *Inorg. Chem.,* 2007, **46**, 2563. (d) G. Hou, L. Bi, B. Li, B. Wang, L. Wu, *CrystEngComm.,* 2011, **13**, 3526. (e) C. H. Zhang, Y. G. Chen, Q. Tang, S. X. Liu, *Dalton Trans.,* 2012, **41**, 9971. (f) M. Zhu, S. Q. Su, X. Z. Song, Z. M. Hao, S. Y. Song, H. J. Zhang, *CrystEngComm.,* 2012, **14**, 6452. (g) F. J. Ma, S. X. Liu, G. J. Ren, D. D. Liang, S. Sha, *Inorg. Chem. Commun.,* 2012, **22**, 174.

3 (a) M. P. Santoni, G. S. Hanan, B. Hasenknopf, *Coord. Chem. Rev.,* 2014, **281**, 64. (b) X. Wang, H. Hu, G. Liu, H. Lin, A. Tian, *Chem. Commun.,* 2010, **46**, 6485. (c) X. Wang, H. Hu, A. Tian, H. Lin, J. Li, *Inorg. Chem.,* 2010, **49**, 10299. (d) A. Yokoyama, T. Kojima, K. Ohkubo, S. Fukuzumi, *Inorg. Chem.,* 2010, **49**, 11190. (e) S. Li, D. Zhang, Y. Y. Guo, P. Ma, X. Qiu, J. Wang, J. Niu, *Dalton Trans.,* 2012, **41**, 9885. (f) Y. N. Chi, P. P. Shen, F. Y. Cui, Z. G. Lin, S. L. Chen, C. W. Hu, *Inorg. Chem.,* 2014, **53**, 5029. (g) Q. Han, X. Sun, J. Li, P. Ma, J. Niu, *Inorg. Chem.*, 2014, **53**, 6107. (h) G. G. Gao, C. Y. Song, X. M. Zong, D. F. Chai, H. Liu, Y. L. Zou, J. X. Liu, Y. F. Qin, *CrystEngComm.*, 2014, **16**, 5150.

4 (a) X. L. Wang, J. Li, A. X. Tian, D. Zhao, G. C. Liu, H. Y. Lin, *Cryst. Growth Des.,* 2011, **11**, 3456. (b) Y. Sawada, W. Kosaka, Y. Hayashi, H. Miyasaka, *Inorg. Chem.,* 2012, **51**, 4824. (c) M. G. Liu, P. P. Zhang, J. Peng, H. X. Meng, X. Wang, M. Zhu, D. D. Wang, C. L. Meng, K. Alimaje, *Cryst. Growth Des.,* 2012, **12**, 1273. (d) J. Q. Sha, J. W. Sun, C. Wang, G. M. Li, P. F. Yan, M. T. Li, *Cryst. Growth Des.,* 2012, **12**, 2242. (e) X. Y. Wu, Q. K. Zhang, X. F. Kuang, W. B. Yang, R. M. Yu, C. Z. Lu, *Dalton Trans.,* 2012, **41**, 11783. (f) Y. Wang, L. M. Wang, Z. F. Li, Y. Y. Hu, G. H. Li, L. N. Xiao, T. G. Wang, D. F. Zheng, X. B. Cui, J. Q. Xu, *CrystEngComm.*, 2013, **15**, 285. (g) X. L. Wang, N. Li, A. X. Tian, J. Ying, T. J. Li, X. L. Lin, J. Luan, Y. Yang, *Inorg. Chem.,* 2014, **43**, 7118.

5 M. Mirzaei, H. Eshtiagh–Hosseini, M. Alipour, A. Frontera, *Coord. Chem. Rev.,* 2014, **275**, 1.

6 (a) M. Mirzaei, H. Eshtiagh–Hosseini, N. Lotfian, A. Salimi, A. Bauza, R. Van Deun, R. Decadt, M. Barcelo–Oliver, A. Frontera, *Dalton Trans*., 2014, **43**, 1906. (b) N. Lotfian, M. Mirzaei, H. Eshtiagh–Hosseini, M. Loffler, M. Korabik, A. Salimi, *Eur. J. Inorg. Chem.,* 2014, 5908.

7 X. Wang, J. Li, H. Lin, G. Liu, A. Tian, H. Hu, X. Liu, Z. Kang, *J. Mol. Struct.,* 2010, **983**, 99.

8 (a) H. Jin, C. Qin, Y. G. Li, E. B. Wang, *Inorg. Chem. Commun*., 2006, **9**, 482. (b) S. L. Li, Y.Q. Lan, J. F. Ma, J. Yang, J. Liu, Y. M. Fu, Z. M. Su, *Dalton Trans*., 2008, 2015. (c) J. Cao, S. Liu, Y. Ren, R. Cao, C. Gao, X. Zhao, L. Xie, *J. Coord. Chem*., 2009, **62**, 1381. (d) X. L. Wang, Z. H. Chang, H. Y. Lin, G. C. Liu, C. Xu, J. Luan, A. X. Tian, J. W. Zhang, *Inorg. Chim. Acta,* 2014, **413**, 16.

9 (a) Y. K. Lu, X. B. Cui, Y. Chen, J. N. Xu, Q. B. Zhang, Y. B. Liu, J. Q. Xu, T. G. Wang, *J. Solid State Chem.,* 2009, **182**, 2111. (b) C. M. Wang, S. T. Zheng, G. Y. Yang, *J. Clust. Sci.,* 2009, **20**, 489. (c) C. L. Meng, P. P. Zhang, J. Peng, X. Wang, Y. Shen, M. G. Liu, D. D. Wang, K. Alimaje, *J. Clust. Sci.,* 2012, **23**, 567.

10 J. Q. Sha, J. W. Sun, C. Wang, G. M. Li, P. F. Yan, M. T. Li, M. Y. Liu, *CrystEngComm.,* 2012, **14**, 5053.

11 APEX2, SAINT, SADABS and SHELXT, Bruker, Madison, WI, USA.

12 Sheldrick, G. M. SHELXL-2014, University of Göttingen, Göttingen, Germany.

13 A. L. Spek, *Acta Cryst.*, 2009, **D65**, 148-155.

14 R. Ahlrichs, M. Bär, M. Hacer, H. Horn, C. Kömel, *Chem. Phys. Lett.*, 1989, **162**, 165–169.

15 S. Grimme, J. Antony, S. Ehrlich, H. Krieg, *J. Chem. Phys.*, 2010, **132**, 154104–19.

16 (a) E. Johnson, S. Keinan, P. Mori–Sánchez, J. Contreras–García, A. Cohen, W. Yang, *J. Am. Chem. Soc*. 2010, **132**, 6498–6506; (b) J. Contreras–García, E. Johnson, S. Keinan, R. Chaudret, J. Piquemal, D. Beratan, W. Yang, *J. Chem. Theory Comput*. 2011, **7**, 625–632; (c) J. Contreras–García, W. Yang, E. Johnson, *J. Phys. Chem. A* 2011, **115**, 12983–12990.

17 L. Z. Zhang, W. Gu, B. Li, X. Liu, D. Liao, Z. *Inorg. Chem.,* 2007, **46**, 622.

18 (a) Q. Yue, J. Yang, G. H. Li, G. D. Li, W. Xu, J. S. Chen, S. N. Wang, *Inorg. Chem.,* 2005, **44**, 5241. (b) P. Mahata, S. Natarajan,

Inorg. Chem., 2007, **46**, 1250. (c) P. Mahata, K. V. Ramya, S. Natarajan, *Chem. Eur. J.,* 2008, **14**, 5839. (d) A. L. Ramirez, K. E. Knope, T. T. Kelly, N. E. Greig, J. D. Einkauf, D. T. De Lill, *Inorg. Chim. Acta,* 2012, **392**, 46.

[19] (a) L. A. GerrardP. T. Wood, *Chem. Commun*., 2000, 2107. (b) W. Chen, H. M. Yuan, J. Y. Wang, Z. Y. Liu, J. J. Xu, M. Yang, J. S. Chen, *J. Am. Chem. Soc.,* 2003, **125**, 9266. (c) Y. K. He, H. Y. An, Z. B. Han, *Solid State Sci.,* 2009, **11**, 49.

[20] Q. Tang, C. J. Zhang, C. H. Zhang, H. Y. Wang, Y. G. Chen, S. X. Liu, *Inorg. Chem. Commun.,* 2012, **15**, 238.

[21] F. A. Carey, *Organic Chemistry*, The Mc Graw–Hill companies, Inc., New York, 1996, pp. 792.

[22] (a) Y. Yao, Q. Cai, H. Kou, H. Li, D. Wang, R. Yu, Y. Chen, X. Xing, *Chem. Lett*., 2004, **33**, 1270. (b) D. Weng, Y. Wang, R. Yu, D. Wang, Q. Cai, H. Li, Y. Yao, *Chem. Lett.*, 2004, **33**, 1586.

[23] (a) C. M. Liu, D. Q. Zhang, D. B. Zhu, *Inorg. Chem. Commun*., 2008, **11**, 903. (b) C. Xie, B. Zhang, X. Wang, B. Yu, R. Wang, G. Z. Shen, *Anorg. Allg. Chem.,* 2008, **634**, 387. (c) X. Liu, H. Nie, L. Wang, R. Huang, *J. Coord. Chem.,* 2013, **66**, 444.

[24] C. X. Zhang, Y. G. Chen, Z. C. Zhang, D. D. Liu, H. X. Meng, *Solid State Sci.,* 2012, **14**, 1289.

[25] (a) X. M. Zhang, M. L. Tong, M. L. Gong, H. K. Lee, L. Luo, K. F. Li, Y. X. Tong, X. M. Chen, *Chem. Eur. J.,* 2002, **8**, 3187. (b) X. M. Zhang, M. L. Tong, X. M. Chen, *Angew. Chem., Int. Ed.,* 2002, **41**, 1029. (c) J. T. Tao, M. L. Tong, X. M. Chen, T. Yuen, C. L. Lin, X. Huang, J. Li, *Chem. Commun*., 2002, 1342.

[26] R. D. Gillard, D. P. J. Hall, *Chem. Commun.,* 1988, 1163.

[27] R. D. Gillard, *Coord. Chem. Rev*., *1975*, **16**, 67.

[28] (a) J. Sha, J. Peng, A. Tian, H. Liu, J. Chen, P. Zhang, Z. Su, Cryst. Growth Des. 2007, 7, 2535. (b) Y. Gao, Y. Xu, Z. Han, C. Li, F. Cui, Y. Chi, C. Hu, J. Solid State Chem. 2010, 183, 1000. (c) Z. Han, T. Chai, Y. Wang, Y. Gao, C. Hu, Polyhedron, 2010, 29, 196.

[29] (a) C. M. Liu, D. Q. Zhang, D. B. Zhu, *Inorg. Chem. Commun*., 2008, 11, 903. (b) W. T. Chen, Y. P. Xu, Q. Y. Luo, X. N. Fang, H. L. Chen, *J. Iran. Chem. Soc.,* 2008, **5**, 484. (c) D. J. Zhang, T. Y. Song, L. Wang, J. Shi, J. N. Xu, Y. Wang, K. R. Ma, W. R. Yin, L. R. Zhang, Y. Fan, *Inorg. Chim. Acta,* 2009, **362**, 299. (d) X. Y. Nie, Q. Z. Li, *Acta Crystallogr., Sect. E,* 2009, **65**, m328. (e) W. T. Chen, *Russ. J. Inorg. Chem*., 2009, **54**, 1230. (f) S. Liu, W. C. Song, L. Xue, S. D. Han, Y. F. Zeng, L. F. Wang, X. H. Bu, *Sci. China Chem.,* 2012, **55**, 1064. (g) E. V. Cherkasova, E. V. Peresypkina, A. V. Virovets, T. G. Cherkasova, *Russ. J. Inorg. Chem.,* 2013, **58**, 1040.

[30] (a) O. R. Evans, W. Lin, *Chem. Matter.,* 2001, **13**, 3009. (b) Z. T. Yu, G. H. Li, Y. S. Jiang, J. J. Xu, J. S. Chen, *Dalton Trans.,* 2003, 4219. (c) C. Xu, S. B. Liu, T. Duan, Q. Chen, Q. F. Zhang, *Z. Naturforsch.,B: Chem. Sci.,* 2011, **66**, 459. (d) J. Wilson, J. Uebler, R. L. LaDuca, *CrystEngComm*., 2013, **15**, 5218.

[31] (a) W. Lin, P. Ayyappan, *Polyhedron.,* 2003, **22**, 3037. (b) K. C. Mondal, O. Senqupta, M. Nethaji, P. S. Mukherjee, *Dalton Trans.,* 2008, 767. (c) C. B. Tian, H. B. Zhang, Y. Peng, Y. E. Xie, P. Lin, Z. H. Li, S. W. Du, *Eur. J. Inorg. Chem.,* 2012, 4029.

[32] (a) J. W. Moore, M. D. Glick, W. A. Baker Jr, *J. Am. Chem. Soc.,* 1972, **94**, 1858. (b) W. Chen, S. Fukuzumi, *Inorg. Chem.,* 2009, **48**, 3800 (c) C. D. Huang, T. R. Qiu, Y. Y. Wu, H. H. Mo, R. H. Zeng, G. Peng, N. Wang, D. S. Lu, Z. Q. Fang, *Z. Anorg. Allg. Chem.,* 2009, **635**, 2381. (d) Z. B. Zhu, H. P. Zeng, *J. Coord. Chem.,* 2010, **63**, 2097.

[33] (a) W. Xiao, X. Gu, D. Xue, *J. Rare Earths,* 2009, **27**, 341. (b) Y. J. Xu, X. X. Yang, H. B. Zhao, *Acta Crystallogr., Sect. E,* 2009, **65**, m310. (c) Z. Hu, Z. B. Zhu, *Acta Crystallogr., Sect. E,* 2009, **65**, m682.

[34] (a) G. A. Bain, J. F. Berry, *J. Chem. Educ.,* 2008, **85**, 532. (b) O. Kahn, *Molecular Magnetism*, Willey–VCH, 1993.

[35] (a) D. Gatteschi, C. Benelli, *Chem. Rev*., 2002, **102**, 2369. (b) Y. Wang, X. L. Li, T. W. Wang, Y. Song, X. Z. You, *Inorg. Chem*., 2010, **49**, 969. (c) M. Andruh, E. Bakalbassis, O. Kahn, J. C. Trombe, P. Porcher, *Inorg. Chem*., 1993, **32**, 1616. (d) J. Chakraborty, A. Ray, G. Pilet, G. Chastanet, D. Luneau, R. F. Ziessel, L. J. Charbonnière, L. Carrella, E. Rentschler, M. S. E. Fallah, S. Mitra, *Dalton Trans.,* 2009, 10263. (e) J. Lhoste, A. Pérez–Campos, N. Henry, T. Loiseau, P. Rabu, F. Abraham, *Dalton Trans.,* 2011, **40**, 9136. f) E. A. Mikhalyova, A. V. Yakovenko, M.s Zeller, K. S. Gavrilenko, S. E. Lofland, A. W. Addison, V. V. Pavlishchuk, *Inorg. Chim.Acta*414, **2014,** 97–104; g) T. D. Pasatoiu, C. Tiseanu, A. M. Madalan, B. Jurca, C. Duhayon,J. P. Sutter and M. Andruh, *Inorg. Chem.*, 50, **2011,** 5879–5889.